

**Fluid inclusion and C and O stable isotopes in hydrothermal calcite from the Gharkohneh iron deposit, NE Iran**Parvin Najafzadeh Tehrani ^{1,*}, Ali Asghar Calagari ¹, Francisco Velasco ²,
Vartan Simmonds ³¹ Department of Earth Science, Faculty of Natural Sciences, University of Tabriz, 5166616471, Tabriz, Iran² Department of Mineralogy and Petrology, Faculty of Sciences and Technology, University of Basque Country UPV/EHU, 48080 Bilbao, Spain³ Research Institute for Fundamental Sciences, University of Tabriz, 5166876393, Tabriz, Iran**ARTICLE INFO**

Submitted: June 2018

Accepted: January 2019

Available on line: February 2019

* Corresponding author:
parvin_tehrani@yahoo.com

DOI: 10.2451/2019PM803

How to cite this article:
Najafzadeh Tehrani P. et al. (2019)
Period. Mineral. 88, 75-91**ABSTRACT**

The Gharkohneh iron deposit is located in the southern Binaloud zone, northeast of Iran. This deposit occurred as lenses, veins/veinlets, and layers of iron oxides and hydroxides within the Devonian carbonates. The main opaque minerals are hematite and goethite, accompanied by lesser amounts of pyrite and magnetite. The hydrothermal calcite is the most important and abundant gangue mineral. It occurs as fine to coarse grains (0.1-4 cm) and is mainly present in the veinlets as well as filling the fracture and intergranular spaces. The $\delta^{13}\text{C}_{\text{(PDB)}}$ and $\delta^{18}\text{O}_{\text{(SMOW)}}$ values of calcite range from -2.6‰ to -8.2‰, and +20.1‰ to +22.3‰, respectively, which are similar to the host carbonates. The C and O isotopic composition of calcite in the host carbonates has become lighter relative to those of the normal Devonian marine carbonates during the formation of iron ores. The microthermometric and isotopic data revealed that late hydrothermal minerals formed as the result of interaction of the hydrothermal fluids with the host carbonates at moderate temperatures (~200 °C) in an open system.

Pyrite and magnetite have been formed by metasomatic replacement of the host carbonates. In contrast, hematite and goethite have been developed during the supergene alteration under oxidizing conditions. Certain convincing evidence such as intimate association of mineralization with fault breccia zone, hydrothermal alteration, and lack of massive sulfide-type ores in the area suggest that the iron deposit in Gharkohneh is of stratabound-type, developed by both hypogene and supergene processes.

Keywords: Hematite; Goethite; Hydrothermal calcite; Fluid inclusion; C and O isotopes; Gharkohneh.

INTRODUCTION

About 4 billion tons of iron ore reserves are known in Iran (Ghorbani, 2013) from various origins, including volcanic, volcanic-sedimentary, magmatic, magmatic-skarn, and sedimentary (Mohseni and Aftabi, 2015) and from different settings and ages (mostly from late Proterozoic to upper Cambrian). Most of these deposits are of volcanic, volcanic-sedimentary, and magmatic origins exemplified by the prestigious apatite-iron oxide deposits

in the Bafq district, central Iran. The latter deposits were envisaged by some researchers to be associated with alkaline magmatism (Forster and Jafarzadeh, 1994; Torab, 2008). However, some other workers envisioned that they are of hydrothermal origin (Jami et al., 2007; Bonyadi et al., 2011; Heidarian et al., 2017). The majority of Mesozoic iron deposits have magmatic-skarn and volcanogenic origins, but those belonging to Cenozoic are affiliated to magmatic processes. Deposits of iron oxide-

apatite with magmatic-hydrothermal origin (Nabatian et al., 2014) in northwest of Iran and the Sangan iron deposit of metasomatic-volcanogenic origin (Boomeri et al., 2010) in east of Iran are two examples of iron deposits related to the Cenozoic magmatic activities.

There are some iron deposits within carbonate and sandstone sedimentary rocks of Paleozoic sequences (Najafzadeh Tehrani et al., 2018a; Najafzadeh Tehrani et al., 2013; Wauschkuhn et al., 1984) in the Binaloud zone, NE Iran. These deposits mainly contain iron oxide minerals and show no direct connection with magmatic rocks, some of which have been formed by supergene processes in the pre-existing hypogene iron-bearing sulfide minerals (Najafzadeh Tehrani et al., 2018b). The primary hypogene iron-bearing minerals are usually missing, but in most cases they have the common mineral assemblage of epithermal stratabound deposits dominated by sulfides (principally pyrite). The most important iron deposits within the Devonian carbonate in NE Iran in the southern part of this zone occurred as veins/veinlets and layers with various thicknesses and are restricted chiefly to areas where the thrust faults are present (Najafzadeh Tehrani et al., 2018a; Wauschkuhn et al., 1984). Some of them are currently being exploited by open-pit method.

As reported by Wauschkuhn et al. (1984) the iron oxides hosted by Devonian carbonates are consisted of several mineralized horizons containing Fe, Pb, and Zn in the middle and upper parts of the Devonian sediments. These workers believed that the submarine volcanic rocks were the potential source for these elements, and that hematite, limonite and Mn-oxides were developed in an oxidizing environment. The recent investigations indicate the presence of magnetite and sulfide veins/veinlets in the ore deposits of this area, which are thought to be formed by acid hypogene hydrothermal fluids (Najafzadeh Tehrani et al., 2018a) and were subsequently affected by intense supergene processes (Najafzadeh Tehrani et al., 2018b).

The Gharkohneh iron deposit with a reserve of approximately 350000 tons of iron-oxide is one of the active small mines in this area which used to be exploited previously by open-pit method. The main portion of this deposit containing iron-oxide ores was formed in the course of supergene processes (Najafzadeh Tehrani et al., 2018b).

This deposit mainly contains goethite and hematite, accompanied by lesser amounts of pyrite and magnetite. The presence of hydrothermal calcite veins/veinlets in the ore zone is regarded to be an important feature of this deposit.

No detailed investigations concerning the genesis of this deposit have been done so far. The current study, however, have been implemented with the aim of determining the mode of formation of this deposit. Owing to the lack of access to the subsurface zones, the focus has been placed

primarily on the hydrothermal calcites collected from the surface outcrops.

In this study, by focusing on C and O stable isotopes in the hydrothermal calcites and the host carbonates, and also relying on the fluid inclusion data obtained from the hydrothermal calcite crystals, we have tried to perceive the origin and physico-chemical characteristics (temperature and salinity) of the ore-forming hydrothermal fluids. The results obtained in this study can help to have better perception of mineralization of other iron deposits and their genetic relationships in this region.

GEOLOGY

Regional geology

The study area is located approximately 80 km southwest of Mashhad, northeast of Iran. Based upon structural division of Iran (Nabavi, 1976; Alavi, 1992), it lies in the southern part of the Binaloud zone (Figure 1).

The Binaloud zone is the eastern prolongation of the Alborz and contains thick sequences of sedimentary, metamorphic and volcanic rocks, along with three generations of thrust faults (Figure 2a). These rocks have a NW-SE trend, which corresponds to that of the Alpine orogeny in Iran. The oldest rocks belong to lower Cambrian and the youngest to Quaternary (alluviums).

The main deformation stage occurred in two periods (Lammerer et al., 1983; Alavi, 1992). The first phase, characterized by strong folding and weak regional metamorphism, happened during the late Variscan-early Kimmerian (middle Jurassic), and the second phase of folding, accompanied by volcanic activity, occurred during the Alpine orogenic phase (Lammerer et al., 1983). Igneous rocks in this region include plutonic (Devonian, Permian, and Jurassic) and volcanic (Eocene-Oligocene). The Devonian basic-ultrabasic plutonic rocks intruded the Silurian sediments (Pourolatifi et al., 2001). The Permian ultramafics are of oceanic lithosphere origin (Lammerer et al., 1983). They consist of basalts and picritic lavas (Holzer and Moemenzadeh, 1969; Davoudzadeh et al., 1975). The lower-middle Jurassic granitoid intruded the Permian-Triassic sediments, and is cropped out in the east of this zone (Alavi, 1991). The Cenozoic volcanic activities include Eocene calc-alkaline andesite, Oligocene-Pliocene dacite (meta-aluminous to peraluminous with moderate potassium), and Miocene-Pliocene alkaline shoshonitic basalts (Spies et al., 1983).

Geology of the study area

The lithologic units include Silurian fine-grained sandstone and Devonian carbonates (Figure 2b). The upper Triassic-lower Jurassic metamorphic rocks unconformably overlie the Silurian and Devonian formations. Faults (normal and strike-slip) and folds

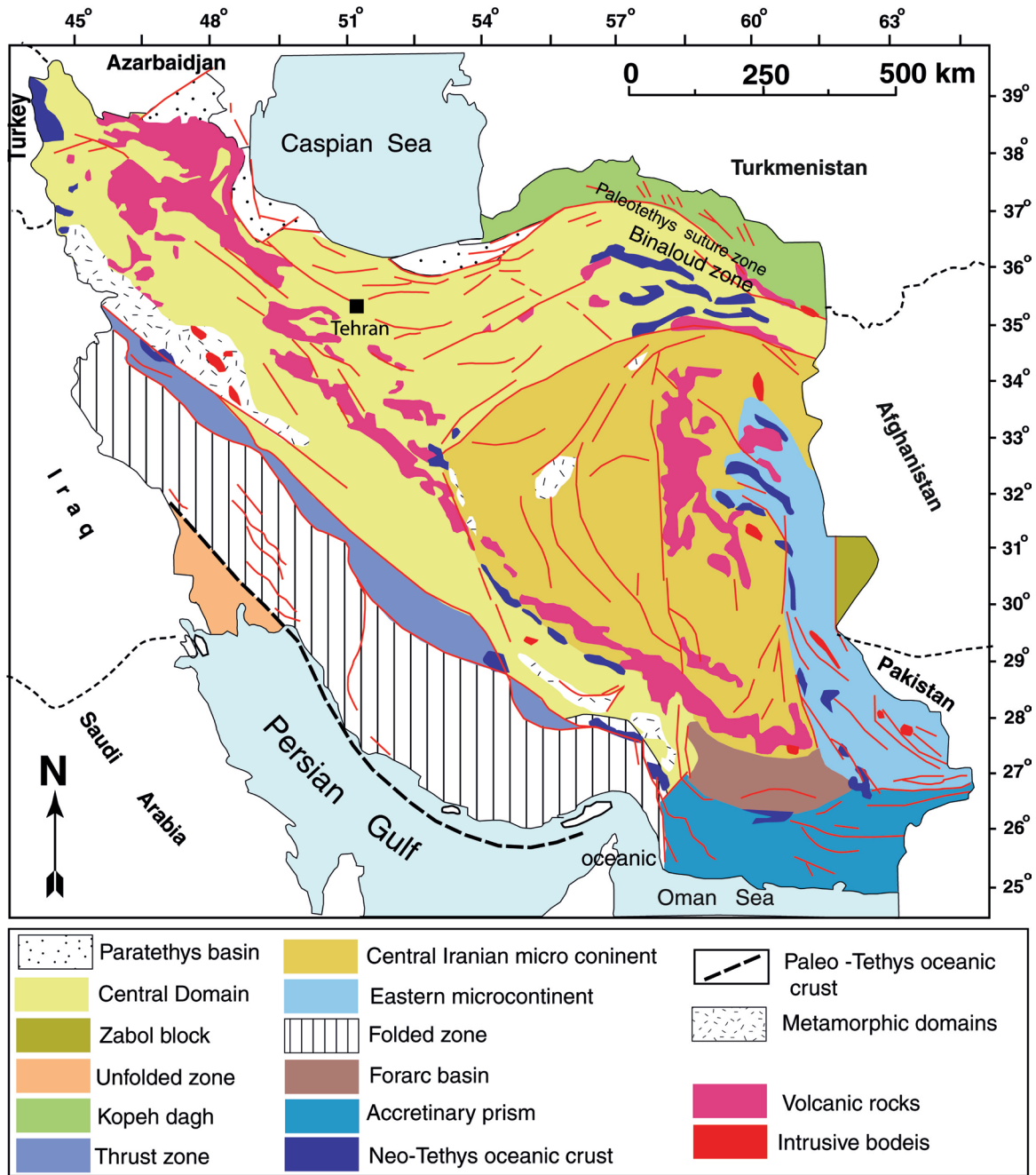


Figure 1. Simplified structural and sedimentary map of Iran and the adjacent regions (after Aghanabati, 2004).

(Figure 3a) are the important structural features at surface. The lower parts of the Devonian sediments contain lenses and layers of iron-oxide ores (Figure 3b).

The Devonian carbonates are thin-layered, belong to a shallow marine environment and suffered a very low degree of metamorphism (Wendt et al., 2005). These rocks are recrystallized, irregularly cross-cut by hematite and calcite veins/veinlets (Figure 4a and 4b) and locally

replaced by hematite in the fault-breccia zone (Figure 3b). Lithologically, these rocks are consisted of limestone and sandy limestone and are karstified in some places, manifested by the solution collapse breccias, whose pore spaces and cavities are filled with hematite and goethite. The limestone is mainly fossiliferous, containing broken fragments of shells and calcite crystals set in a micritic calcareous matrix. Based upon classification of Folk

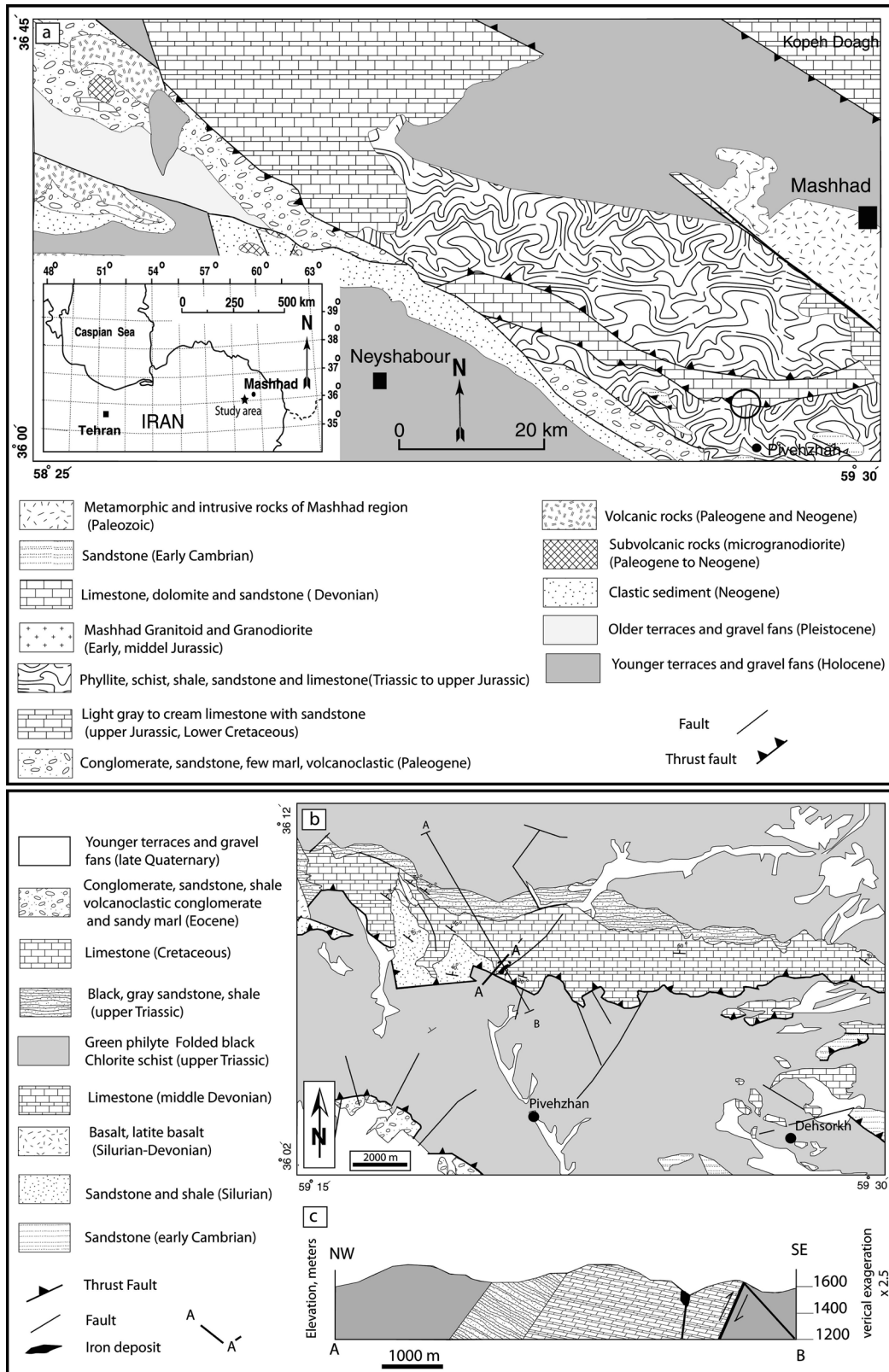


Figure 2. a) The geological map of Binaloud zone modified after Lammerer et al. (1983). The study area is shown in the bottom left corner of the quadrangle (plain circle), b) Geological map of the study area encompassing the iron deposit in the southern Binaloud zone, SW Mashhad (after Pourlatifi et al., 2001), c) Cross section of the Gharkohneh iron deposit.

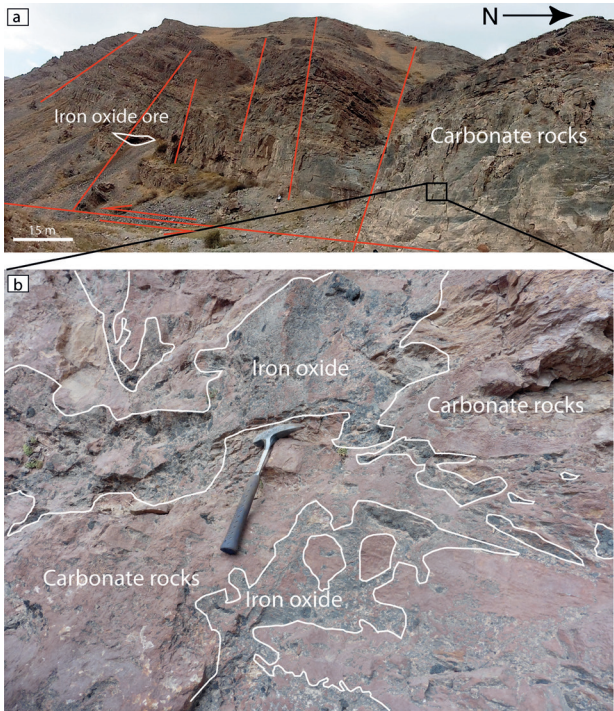
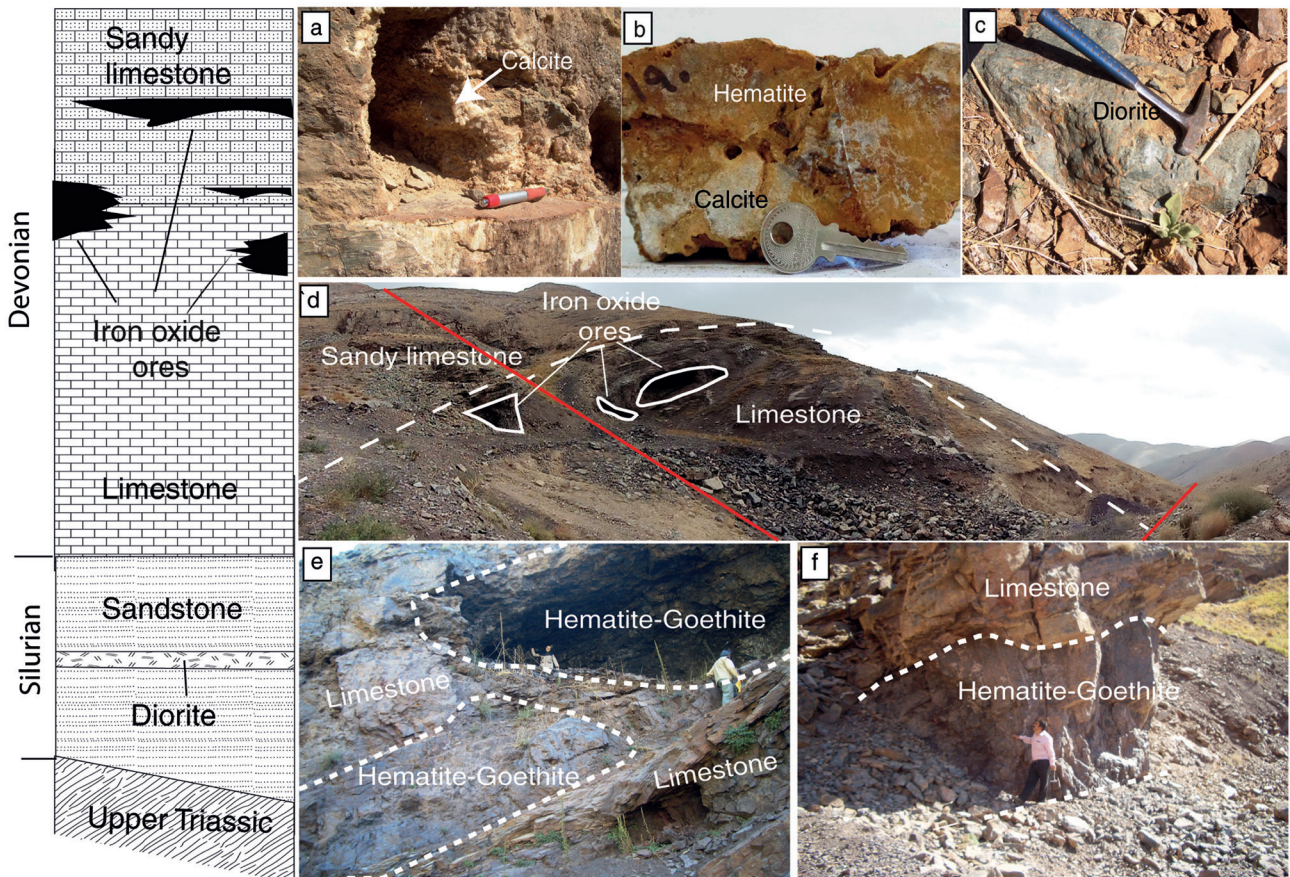


Figure 3. a) Field photographs exhibiting the Devonian carbonates in the study area (looking toward west). Shown in this photograph are also the structural features (folding and faulting) in carbonate units. Iron mineralization occurred in fault zones (shown in red lines), b) Replacement of carbonates by iron oxide along the fault breccia zone.

Figure 4. Field and hand specimen photos together with the schematic stratigraphic column across the studied profile in the Gharkohneh area. a) Calcite veins within the carbonates host rocks, b) Hydrothermal calcite veinlets developed within secondary hematite ores, which in turn were resulted from oxidation of primary sulfides (pyrite) in the Devonian carbonates, c) Small patches of porphyry diorite cropping out within the Silurian sandstone in ~700 km west of the study area, d) Stratabound iron ores appearing as massive bodies and lenses in the folded and karstified carbonate. Fault is shown by red lines, e) Open space filling by iron ores, f) Massive layers of iron ores.

Schematic stratigraphic column of Gharkohneh area (A – A' across travers)



(1962), it varies from biomicrite to dismicrite. The sandy limestone is dark green to gray in color and consists of calcite, muscovite, monocrystalline quartz and Fe-oxides.

There are a few dispersed and small patches of subvolcanic intrusive bodies (Figure 4c) cropping out within the Silurian sandstone in approximately 700 m west of the study area. They are unmineralized and have no direct connection with the Gharkohneh iron deposit. These rocks have dioritic compositions and on the basis of textural evidence were emplaced in shallow depth.

They have creamy gray color in fresh outcrops, but vary in color from light green to dark where suffered intense hydrothermal alteration. Mineralogically, they consist of quartz, plagioclase, pyroxene and biotite. Plagioclase occurs mainly as phenocrysts and is partially replaced by sericite. The pyroxene and biotite were partially altered to calcite and chlorite, respectively. The presence of chlorite imparts a green color to this rock. Hematite is the only opaque mineral present in this rock.

HYDROTHERMAL ALTERATION AND MINERALIZATION

The Gharkohneh iron deposit is stratabound (Figure 4d) and the ores occurred as open-space fillings, veins/veinlets, lenticular massive bodies (Figure 4e and 4f), and concordant layered masses in the host carbonate rocks. The lenticular and the massive ores are irregular having 10-200 m length and 5-10 m width and consist mainly of goethite, (displaying colloform and botryoidal textures) and hematite (showing boxwork texture), accompanied by subordinate amounts of dispersed magnetite and pyrite. These ores were cut by calcite veinlets. The layered ores have up to 1 m width and consist chiefly of hematite.

The iron ores within veins/veinlets contain hematite and goethite having variable thicknesses (1-100 cm). The veinlets of the secondary pyrite and calcite cut into the carbonate host rocks.

The replacement of the host carbonates by the Fe-oxide along the bedding planes and occurrence of mineralization in the fault and fractured zones are the most important features indicating an epigenetic origin. The substantial replacement of carbonates by iron-oxides testifies to the intense chemical interaction between the ore-bearing solution and the host minerals during the mineralization processes. Since mineralization mainly occurred as veins/veinlets and open-space fillings, it can be deduced that the secondary permeability and reaction with wall rocks have played a crucial role in magnetite and sulfide deposition.

Hematite shows skeletal, micaceous (foliated), and boxwork textures (Figure 5a), while goethite chiefly displays botryoidal and colloform textures. Magnetite occurs as fine-grained (20-50 μm) anhedral to euhedral crystals (Figure 5b), and is mostly disseminated and often martitized.

Fine to medium-grained pyrite crystals occurred as veinlets within the host carbonates and also is sporadically dispersed within the iron ores (Figure 5a) and carbonate host (Figure 5c and 5d). They were altered to goethite and hematite and pseudomorphs of goethite after pyrite are quite common. Fine to coarse-grained (0.1-4 cm) calcite crystals occurred as veins/veinlets, filling the interstitial spaces and cavities within the iron ores (Figure 4b) and host rocks (Figure 5e), and coexist with subhedral secondary Fe-sulfides which were oxidized to hematite (Figure 5f). The coarse crystals exhibit twinning and triple junction pattern (Figure 5g).

Considering field relations and petrographic examinations, this deposit has been formed during two distinct episodes of alteration, (1) hypogene and (2) supergene.

Based upon petrographic examinations and XRD analyses, the hypogene hydrothermal alteration can be temporally divided into two stages, (1) the early and (2) the late (Figure 6). The early stage was accompanied by the formation of magnetite±pyrite±sericite±quartz which occurred as dissemination and veins/veinlets within the sandy limestone. During the late stage of hypogene alteration, minerals such as pyrite±calcite were developed. The supergene alteration, however, is characterized by the development of minerals like hematite±goethite±pyrolusite±gypsum (Figure 6).

During the first stage of hypogene mineralization the infiltration of hydrothermal solutions in the host rocks brought about sericitic alteration and deposition of disseminated magnetite and pyrite. The presence of remnants of minerals such as quartz, sericite, magnetite, and pyrite indicates the influence of hydrothermal solutions on the host rocks (Figure 5c). This alteration halo is observable up to about 50 meters far away from the mineralized zones.

The magnetite of the early hypogene stage was likely formed by the reaction of high-temperature acid solutions (<300 °C; Barnes, 1997) with the enclosing carbonate rocks and the consequent increase in pH (Barnes, 1997). Formation of magnetite was accompanied by the reduction of sulphate to sulphide in the hydrothermal fluids (Barnes, 1997), giving rise to the formation of sulfides (pyrite). Nonetheless, determination of the precise mode of formation of this mineral requires access to the subsurface zones.

The second generation of pyrite along with hydrothermal calcite were precipitated as veinlets and open-space fillings during the late stage of hypogene mineralization. The hydrothermal calcite was formed following the reaction of oxidized carbon species (including H_2CO_3 and HCO_3^-) with Ca-bearing minerals in the host rocks (Zheng, 1990).

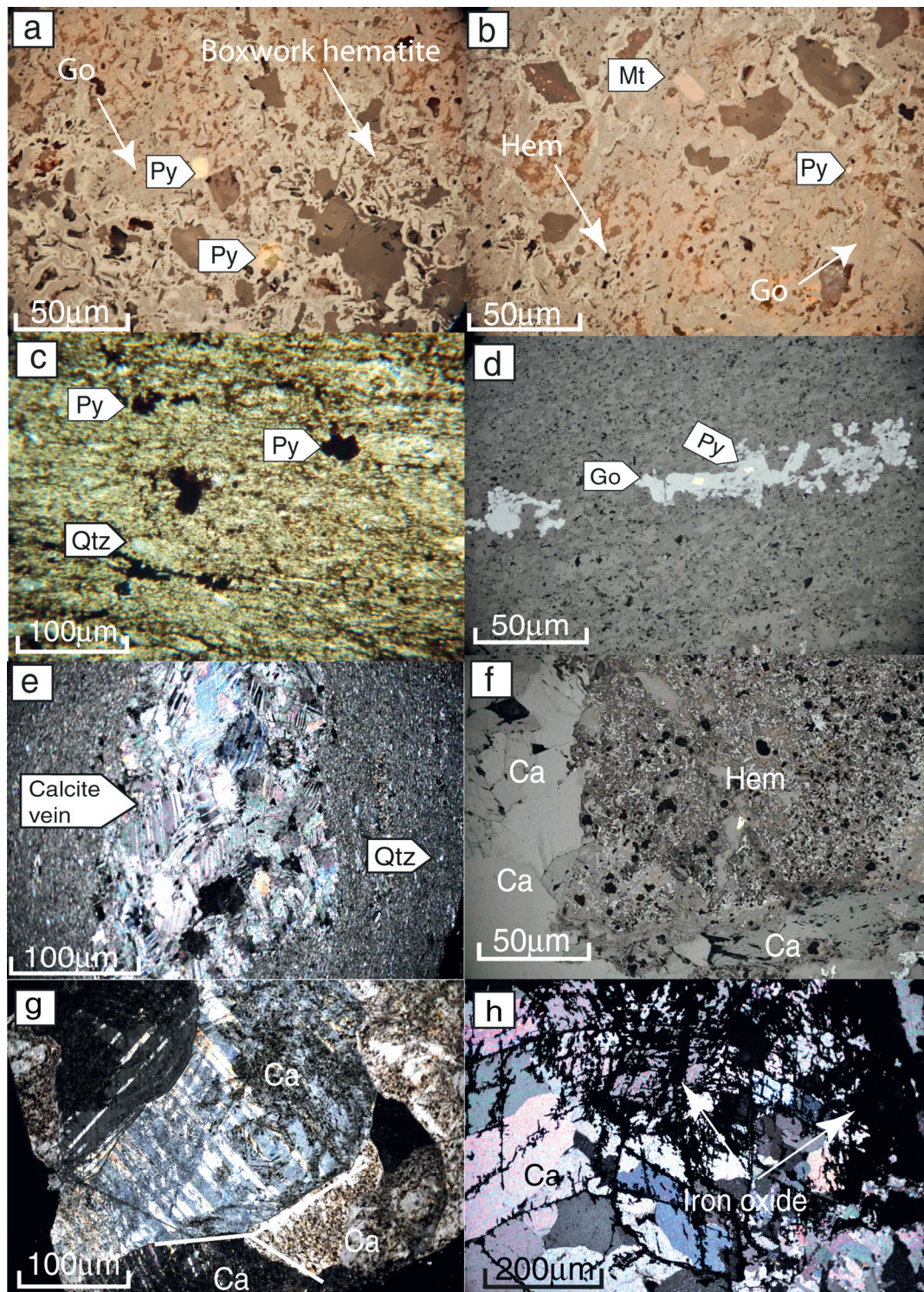


Figure 5. Photomicrographs of the iron ores. a) Hematite shows skeletal and boxwork textures and pyrite is present as relict islands within the goethite, b) Euhedral magnetite crystals dispersed within hematite and goethite, c) Euhedral pyrite in sandy limestone which suffered sericitic hydrothermal alteration, d) Pyrite and pseudomorph of goethite after pyrite in veins and veinlets of carbonate host rock, e) Hydrothermal calcite veinlet within the carbonate host rock, f) Coexistence of calcite and subhedral secondary Fe-sulfides which were oxidized to boxwork hematite, g) Coarse-grained calcite crystals showing twinning and triple junction pattern, h) Network replacement texture in hydrothermal calcite. Calcite crystals were replaced by hematite along the cleavage and twinning planes. Hem=hematite, Go=goethite, Mt=magnetite, Py=pyrite, Ca=calcite, Qtz=Quartz.

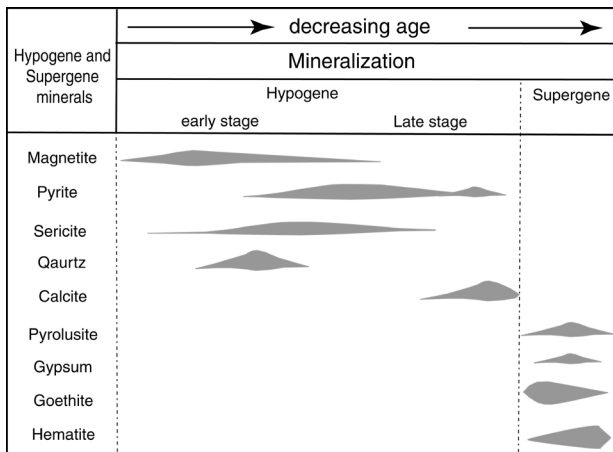


Figure 6. Paragenetic sequences of the ore and gangue minerals in the Gharkohneh iron ores.

The primary porosity in the host carbonates along with the secondary porosity generated by faulting and fracturing facilitated the penetration and percolation of the oxidizing supergene solutions through the hypogene sulfide ore zones. Textural examinations showed that the hydrothermal calcite crystals were replaced initially by hematite along the cleavage and twinning planes (Figure 5h). Then, the replacement advanced as interpenetration and irregular patterns within the crystals by gradual progression of mineralization, which finally engulfed the entire crystal.

METHOD OF INVESTIGATION

Five iron ore samples were chemically analyzed by Wavelength Dispersive X-ray Fluorescence (WDXRF) method [for determining major (as wt%) and minor (As, Ba, Co, Cu, Cr, F, Mo, Ni, Nb, Pb, Rb, S, Sr, V, W, Y, Zn, Zr, Cs, Th, Sn; as ppm)] elements using a PANalytical Axios Advanced PW4400 XRF spectrometer (4 kW Rh anode SST-mAX X-ray tube) at the SGiker laboratories (UPV/EHU, Spain). Fused beads were prepared by mixing 0.2 g of finely ground sample with 3.8 g of a lithium borate flux (Spectromelt A12, Merck) and LiBr as non-wetting agent. The lower detection limit for major and minor elements is ~0.01 wt% and ~5 ppm, respectively. In addition, five samples of the iron ores were chemically analyzed for trace elements using ICP-AES methods (Model 737 Series, Agilent-Varian, Australia) in the Iranian Mineral Processing Research Center, Karaj. Samples were prepared on the basis of ASTM D4898 standard. After pulverizing, about 0.25-1 g of the each sample was treated by "Four Acid Digestion" method using HF, HCl, HNO₃, and HClO₄, which can fully decompose the sample. Then, the obtained solution was diluted to a standard volume by distilled water and finally was injected into the analyzing instrument. Lower limit of detection for major elements

(P, Ca, Fe, K, Mg, Na, Mg, Ti, Al, S) are in the range of 0.01 wt%, 2 ppm for trace elements (Ce, Co, Cr, Cu, La, Mn, Ni, Pb, Sb, Sc, V, Zn, As, Bi, Sr, Li, Y, Be, Ag, Cd, Mo), and 0.05 wt% for S.

Four samples from the host carbonates and six of the hydrothermal calcites coexisting with iron-oxides were analysed for C and O stable isotopes (using MAT-253 continuous spectrometer) in the laboratory of the Spanish National Research Council, Madrid (Spain). Carbonate samples were converted into CO₂ by reaction with phosphoric acid at 25 °C, and the produced CO₂ was analysed on the mass spectrometer. All the analytical raw data were corrected using standard procedures (Craig, 1957) and reported in standard δ -notation as permil (‰) deviations relative to the Vienna Standard Mean Ocean Water (V-SMOW) and Pee Dee Belemnite (PDB) standards. Typical errors of reproducibility, 1s, were $\pm 0.1\%$ for $\delta^{13}\text{C}_{\text{PDB}}$ and $\pm 0.2\%$ for $\delta^{18}\text{O}_{\text{SMOW}}$.

Doubly polished wafers (~100 μm thick) were prepared of samples taken from the calcite veinlets (8 samples) containing boxwork hematite and remnants of pyrite in the main part of the deposit. Fluid inclusion studies were mainly performed on calcite crystals. The isotopic analyses were also carried out on the same samples. The salinity and homogenization temperature (T_{H}) of the fluid inclusions were measured by using Linkam-THMS-600 stage in Iranian Mineral Processing Research Center, Karaj (Iran). The stage was equipped with two heating (TP94) and freezing (LNP) controllers attached to an Olympus petrographic microscope and a video monitoring system. The temperature range for the instrument was from -196 °C to +600 °C. Also this instrument was equipped with controllers for heating (TP94) and cooling (LNP), nitrogen tank (for cooling and super-cooling), and water tank (for cooling at high temperatures). For calibrating the instrument (stage), the following standards were used:

Heating: Cesium nitrate, melting point: +414 °C

Freezing: n-Hexane, melting point: -94.3 °C

The data are reproducible to ± 0.6 °C for heating runs and ± 0.2 for freezing runs.

Upon progressive heating, up to 3 phase transitions were observed in the inclusions, namely eutectic melting (T_{e}), ice melting [$T_{\text{m(ice)}}$], and total homogenization temperatures [$T_{\text{H(Total)}}$]. The bulk salinity of the fluid was calculated from $T_{\text{m(ice)}}$ (Steele-MacInnis et al., 2011).

GEOCHEMISTRY

Behavior of the major and minor elements during the formation of iron ores at Gharkohneh was investigated by analyzing ten goethite-hematite ore samples (Table 1). Based upon geochemical data obtained from the iron ore samples, the average concentration values of major and minor elements are as follows:

$\text{Fe}_2\text{O}_3=78$ wt%, $\text{MnO}=2$ wt%, $\text{Cu}=409$ ppm, $\text{Pb}=72$ ppm, $\text{Zn}=64$ ppm, $\text{Co}=18$ ppm, and $\text{Ni}=22$ ppm.

MICROTHERMOMETRIC STUDY

Fluid inclusion studies were carried out on the vein/veinlet calcite crystals coexisted with remnants of secondary pyrite and boxwork hematite within the veinlets cutting into the primary ores (Figures 4b, 5f and 5g) which are thought to be formed during the late stage of hypogene alteration and mineralization processes. Most of the analyzed fluid inclusions are irregular, elongate, polygonal, and rarely rhombic in shape and vary in size from 7 to 30 μm (Figure 7a and 7b). The majority of the fluid inclusions are primary and liquid-rich 2-phase (L+V). The V_L in these fluid inclusions vary from 50% to 70%.

The microthermometry results show that the last ice melting temperatures ($T_{m_{ice}}$) range from -16.3 °C to -0.3 °C, which correspond to the salinity range of 0.21-12.59 wt% NaCl_{eq} . (listed in Table 2). However, most of the inclusions have salinities ranging from 0.21 to 6 wt% NaCl_{eq} . (Figure 8a). The measured eutectic temperatures were generally around -22 °C implying mainly a $\text{NaCl}-\text{H}_2\text{O}$ system. Since no clathrate ($\text{CO}_2 \cdot 6\text{H}_2\text{O}$) was recognized in the analyzed fluid inclusions, it can be inferred that the CO_2 content of the fluids was less than 2.7 wt% (Hall et al., 1988).

Almost all inclusions homogenized by vapor disappearance had homogenization temperatures (T_H) within the range of 141-231 °C. However, most of the data points cluster in the range of 180-200 °C (Figure 8b). In general, no significant variation in salinity was observed with the increasing of T_H . The estimated densities for these inclusions vary from 0.8-0.98 g/cm^3 (Figure 9).

Table 1. Chemical analysis results of the iron ore samples obtained by the XRF+ ICP(OES) methods.

	n	Min	Max	Mean
SiO_2 wt%	5	0.96	3.16	1.85
Al_2O_3	10	0.28	3.02	1.36
Fe_2O_3	5	63.0	89.4	78.2
MnO	10	0.94	3.49	2.21
MgO	10	0.00	6.47	1.12
CaO	10	0.48	18.61	8.59
Na_2O	5	0.00	0.28	0.10
K_2O	10	0.01	0.72	0.22
TiO_2	10	0.00	0.08	0.05
P_2O_5	5	0.01	0.03	0.02
As (ppm)	10	0.00	296	97.5
Co	5	14.0	34.0	18.0
Cu	10	30.0	1493	409
Ni	3	14.5	34.0	22.4
Pb	10	44.0	134	72.0
S	10	129	2800	1679
Zn	10	34.0	95.6	63.7
V	7	20.0	65.4	46.0
Cr	7	12.0	77.0	51.6

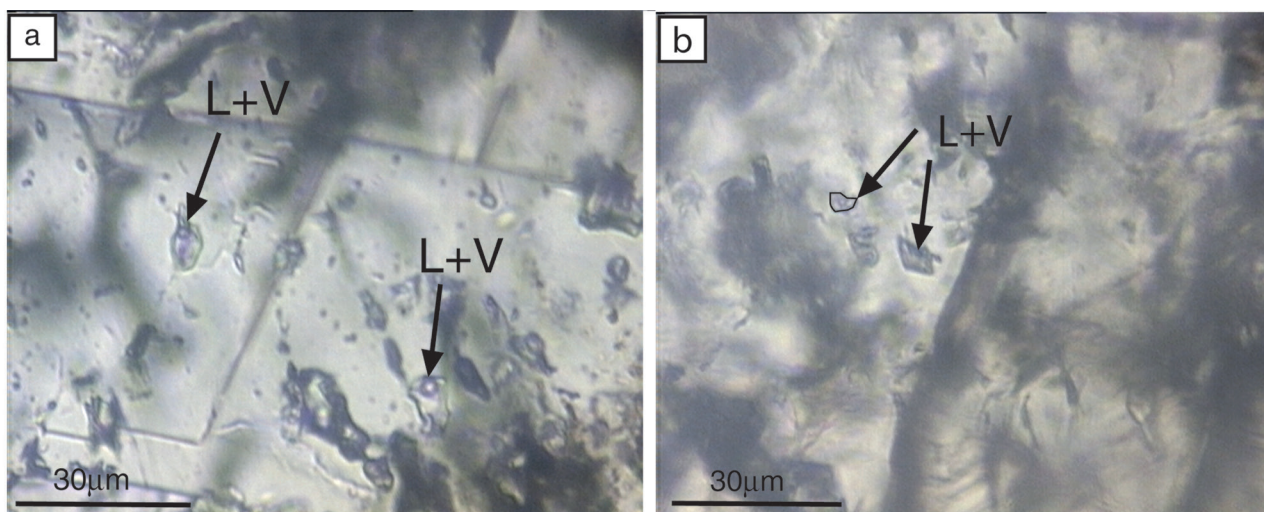


Figure 7. Morphologies and shapes of various liquid-rich 2-phase fluid inclusions in the hydrothermal calcite crystals, including spherical, irregular, and polygonal shapes.

Table 2. Collected microthermometric data obtained from fluid inclusions in vein/veinlet hydrothermal calcite. Salinity is expressed as wt% NaCl_{eq}. T_{m(ice)}: temperature of final ice melting; T_H: Homogenization temperature.

Sample	Inclusion type	Size (μm)	T _{m(ice)} (°C)	T _{H(L-V)} , °C	Mode	wt% NaCl _{eq}
1	Primary L+V	30	-9.0	180	L+V=>L	8.42
2	Primary L+V	20	-10.1	190	L+V=>L	10.1
3	Primary L+V	15	-9.2	185	L+V=>L	8.54
4	Primary L+V	10	-15.0	182	L+V=>L	12.1
5	Primary L+V	15	-16.3	184	L+V=>L	12.6
6	Primary L+V	15	-1.9	231	L+V=>L	3.21
7	Primary L+V	10	-1.1	172	L+V=>L	1.76
8	Primary L+V	7	-2.5	190	L+V=>L	4.24
9	Primary L+V	7	-0.3	220	L+V=>L	0.21
10	Primary L+V	15	-2.5	161	L+V=>L	4.00
11	Primary L+V	10	-15.0	188	L+V=>L	12.3
12	Primary L+V	12	-11.0	191	L+V=>L	11.2
13	Primary L+V	10	-4.3	141	L+V=>L	7.07
14	Primary L+V	8	-1.9	186	L+V=>L	3.21
15	Primary L+V	15	-0.4	209	L+V=>L	0.4
16	Primary L+V	15	-0.3	200	L+V=>L	0.21
17	Primary L+V	17	-0.3	201	L+V=>L	0.21
18	Primary L+V	12	-0.3	180	L+V=>L	0.21
19	Primary L+V	15	-0.4	190	L+V=>L	0.21
20	Primary L+V	7	-0.7	208	L+V=>L	0.99
21	Primary L+V	5	-1.7	142	L+V=>L	1.86
22	Primary L+V	20	-3.1	141	L+V=>L	5.23
23	Primary L+V	30	-0.4	150	L+V=>L	0.40
24	Primary L+V	8	-3.0	157	L+V=>L	5.07
25	Primary L+V	12	-2.5	157	L+V=>L	4.24

Table 3. Oxygen and carbon isotopic data for the host carbonates and hydrothermal calcite. Ca: calcite, Go: goethite, Hem: hematite, Qtz: quartz, Mus: muscovite.

Sample ID	Sample type	Associated mineral (s)	δ ¹³ C (‰, VPDB)	δ ¹⁸ O (‰, SMOW)
13	Hydrothermal calcite	Ca, Go	-4.5	20.1
16	Hydrothermal calcite	Ca, Hem	-4.1	21.8
186	Hydrothermal calcite	Ca, Go, Hem	-5.9	21.7
189	Hydrothermal calcite	Ca	-2.8	20.4
190	Hydrothermal calcite	Ca, Go	-2.6	22.3
198	Hydrothermal calcite	Ca	-8.2	22.2
12	Sandy limestone	Ca, Qtz, (+Mus)	-2.5	21.9
194	Sandy limestone	Ca, Qtz, (+Mus)	-2.3	21.0
2	Limestone	Ca, Qtz	-3.1	20.2
200	Limestone	Ca, Qtz	-5.0	21.1

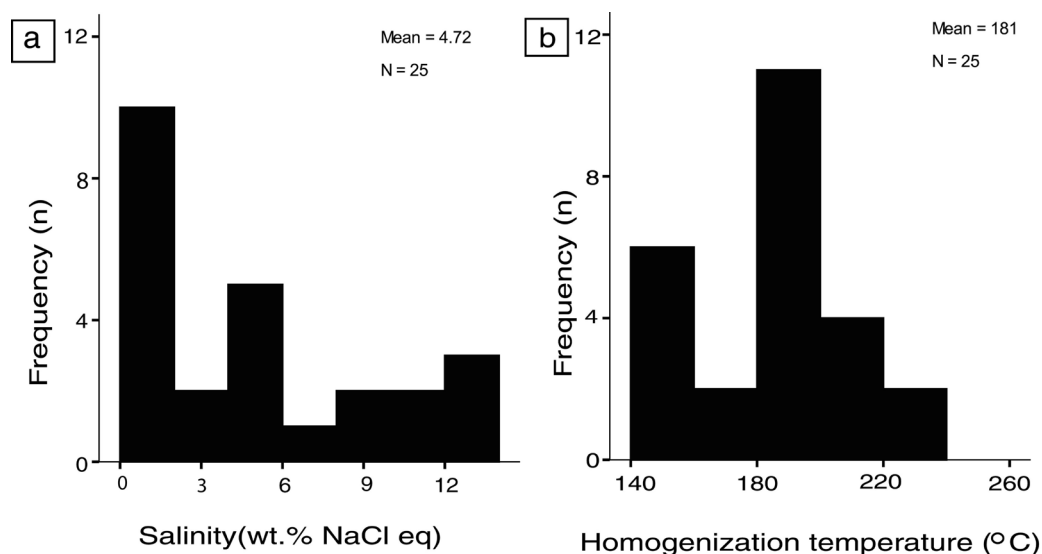


Figure 8. Histograms of (a) salinity and (b) homogenization temperature (T_H) for the liquid-rich 2-phase fluid inclusions in the hydrothermal calcite crystals.

Since the pressure corrections have not been done, the obtained T_H is the minimum temperature at which the ore minerals have been formed. Fluid inclusion data points in such a plot lie within the epithermal field (Figure 9).

OXYGEN AND CARBON STABLE ISOTOPES

Two samples from the limestone, two from the sandy limestone and six from the calcite veinlets were measured for C and O stable isotopes, results of which ($\delta^{13}C_{PDB}$ and $\delta^{18}O_{SMOW}$) are listed in Table 3.

Carbon isotope

The isotopic composition of carbon ($\delta^{13}C_{PDB}$) in the limestone and sandy limestone varies from -3.1‰ to -5.0‰ and from -2.3‰ to -2.5‰, respectively, which is lighter than the Devonian carbonates (with the mean of +0.4‰; Keith and Weber, 1964).

The $\delta^{13}C_{PDB}$ values in calcite veins/veinlets vary from -2.6‰ to -8.2‰ with an average of -4.7‰.

Oxygen isotope

The isotopic composition of oxygen ($\delta^{18}O_{SMOW}$) in the limestone and sandy limestone units varies from +20.2‰

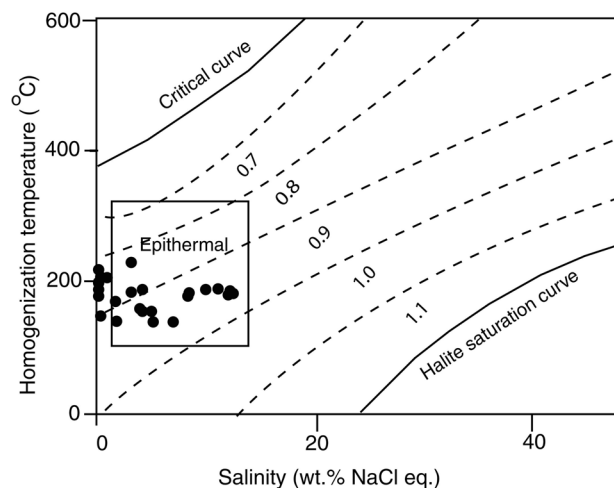
to +21.1‰ and from +21.0‰ to +21.9‰, respectively. These ranges are lighter than Devonian carbonates (with the mean of +23.5‰; Keith and Weber, 1964).

The oxygen isotopic composition ($\delta^{18}O_{SMOW}$) of the hydrothermal calcite varies from +20.1‰ to +22.3‰ (mean of +21.42‰), which is almost similar to the corresponding values of the host rocks.

DISCUSSION

Studying the carbon and oxygen isotopic composition of carbonate minerals, especially the hydrothermal calcite, is one of the practical geochemical methods for recognizing the origin of ore-forming fluids in metallic deposits (Zheng and Hoefs, 1993; Fernández-Nieto et al., 2003; Torres, 2006; Boomeri et al., 2010; Taofa et al., 2011;

Figure 9. Bivariate plot of the homogenization temperature (T_H) versus salinity (expressed as wt% NaCl_{eq.}). Shown in this figure are the halite saturation curve and the critical curve (Ahmad and Rose, 1980), as well as the typical ranges for inclusions from epithermal deposits (Wilkinson, 2001). Moreover, iso-density (g/cm³) curves of the NaCl-H₂O system are also shown (Wilkinson, 2001), which represent the data generated by the equation-of-state of Zhang and Frantz (1987).



Zhou et al., 2014). Variations in the isotopic composition of C and O in the hydrothermal calcite usually occur as the result of (1) mixing of two different solutions leading to calcite precipitation, (2) fluid-rock interaction, which causes direct precipitation of calcite, and (3) alteration of primary calcite (Zheng, 1990). Variables controlling the isotopic composition of the hydrothermal calcite include composition of the incipient fluid, temperature, and the carbon species present in the fluid (Zheng and Hoefs, 1993).

Since temperature has enormous effect on isotopic fractionation during the precipitation of calcite from solution, the mixing processes can be deduced from carbon and oxygen isotopic data (Zheng and Hoefs, 1993). The isotopic composition of a fluid can considerably change due to fluid/rock interaction during its migration through the wall rocks (Zheng and Hoefs, 1993).

The isotopic composition of carbon ($\delta^{13}\text{C}_{\text{PDB}}$) in the carbonate host rocks is relatively lighter than the Devonian carbonates worldwide (with the mean of +0.4‰; Keith and Weber, 1964) (Figure 10). The sensible variation in $\delta^{13}\text{C}$ of carbonate rocks occurs as the result of minor changes in pH and $f\text{O}_2$ (Ohmoto and Rye, 1979; Ohmoto, 1986), and/or dissolution of carbonates (Ohmoto, 1972), which commonly lead to the increasing of light carbon. It seems that decarbonation of the marine limestone during hydrothermal metasomatism has caused the $\delta^{13}\text{C}_{\text{PDB}}$ decrease. The relatively lighter carbon of the vein calcite in comparison with the host carbonates is probably due to the interaction of hydrothermal fluids with the host rocks during the mineralization and processes.

The isotopic composition of oxygen ($\delta^{18}\text{O}_{\text{SMOW}}$) in the host carbonate units is lighter than the published values from Devonian carbonates worldwide (Figure 10).

This was probably resulted from dissolution of the host carbonates by hydrothermal fluids, leading to a sensible decreasing in the original $\delta^{18}\text{O}_{\text{SMOW}}$ value. The $\delta^{18}\text{O}$ values are lower (ranging from 3.3‰ to 1.6‰) than those of the Devonian carbonates (with the mean of +23.5‰; Keith and Weber, 1964). Therefore, it seems that the primary composition of $\delta^{18}\text{O}_{\text{SMOW}}$ suffered a decrease of 1.6‰ to 3.3‰ during the interaction of hydrothermal fluids with the host carbonates.

Finally, the similarities between the $\delta^{13}\text{C}_{\text{PDB}}$ and $\delta^{18}\text{O}_{\text{SMOW}}$ values of the hydrothermal calcite and those of the host rocks also suggest that the hydrothermal fluids were isotopically in equilibrium with the host rocks and the CO_2 of the ore-forming fluids was mostly derived from dissolution of the host carbonates.

Water-rock interaction model

Variation in carbon and oxygen isotopic values of the hydrothermal calcite and the host carbonates could be due to the isotopic exchange during the water-rock interaction. With the advance of water-rock isotopic exchange reactions, oxygen and carbon isotopic values decrease progressively. Processes like CO_2 -degassing and calcite precipitation from solution can have considerable effect on isotopic values of the fluids (Zheng, 1990).

Although liquid CO_2 has not been detected in our fluid inclusion study, fluids when its content is below 1.0 mole% in epithermal it would not appear as an immiscible liquid phase in fluid inclusions (Bodnar et al., 1985). Thus, despite the lack of evidence for the occurrence of boiling, it is still possible that hydrothermal fluids did have sufficient CO_2 to release gradually.

Figure 11 shows the fluid/rock interaction model for open and closed systems.

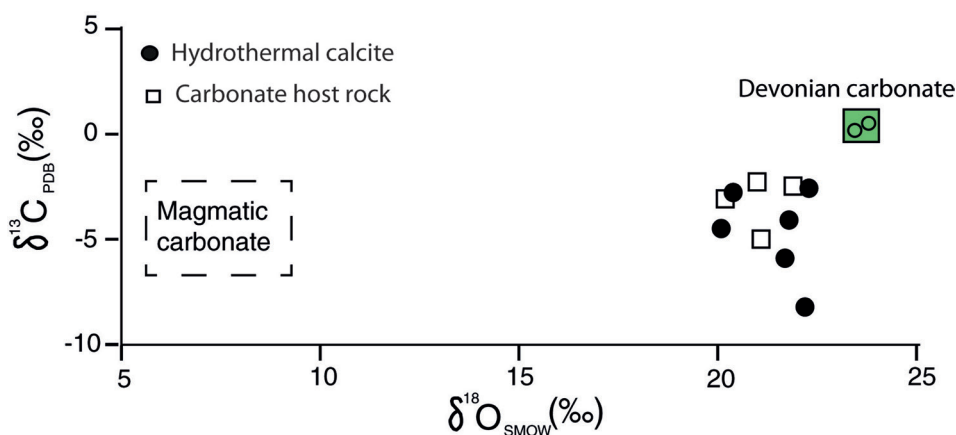


Figure 10. Bivariate plot of $\delta^{13}\text{C}_{\text{PDB}}$ versus $\delta^{18}\text{O}_{\text{SMOW}}$ of the carbonate host rocks and hydrothermal calcite. Data points are clustered close to the marine carbonates. Data of the Devonian carbonates are from Keith and Weber (1964) and those of the magmatic carbonates are from Taylor et al. (1967).

In this way, the diagram can be used for estimation of water-rock mixing rate in open and closed systems, evaluation of temperature variation, and estimation of the H₂CO₃ content in the hydrothermal fluids.

For calculation of the isotopic composition variations in hydrothermal calcite and the host carbonates, the following equations (1 and 2) were applied.

$$\text{CaCO}_3\text{-H}_2\text{CO}_3: 1000\text{Ln}\alpha = 3.73(10^6/T^2) - 9.81 \cdot 10^3/T + 3.72 \quad (1)$$

(Bottinga, 1969)

$$\text{CaCO}_3\text{-H}_2\text{O}: 1000\text{Ln}\alpha = 2.78(10^6/T^2) - 3.39 \quad (2)$$

(O'Neill et al., 1969)

The parameters in equation 1 and 2 include the original values of carbon and oxygen isotopes, which belong to

unaltered Devonian carbonates worldwide (Keith and Weber, 1964). H₂CO₃ was presumed to be the dominant species in hydrothermal fluids. Since the δ¹³C values of the hydrothermal calcite are between -2.5‰ and -8.2‰, the presence of H₂CO₃ in the hydrothermal fluids at Gharkohneh seems evident.

Considering the values of δ¹⁸O of the veinlet calcite (about +21.4‰) and the temperatures measured by microthermometric analyses (180-200 °C), it can be suggested that hydrothermal fluids could have δ¹⁸O values between +8‰ and +10‰. This range is near the typical composition of the magmatic fluids. Accordingly, the carbon composition of the assumed (variably modified) magmatic fluids should be ranging from -13‰ to -3‰ with a mean of about -8‰ (Rye and Ohmoto, 1974; Ohmoto and Rye, 1979).

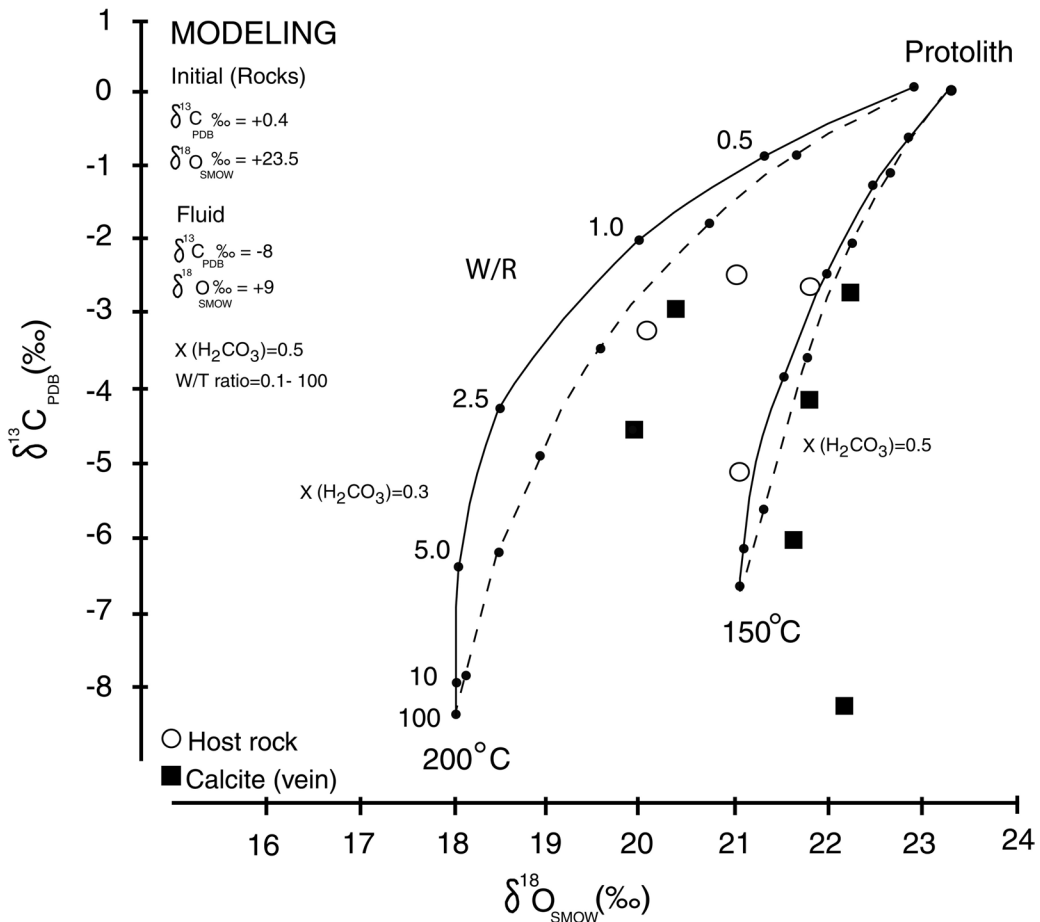


Figure 11. Fluid/rock interaction model in bivariate plot of δ¹⁸O versus δ¹³C on which, data points of the Gharkohneh iron ores and two lines reflecting the fluid/rock ratios at two different temperatures (150 °C and 200 °C) are shown (Zheng and Hoefs, 1993). Moreover, the isotopic composition of C and O for Devonian marine carbonates as parent rocks (δ¹⁸O_{SMOW}=23.5‰ and δ¹³C_{PDB}=+0.4‰; Keith and Weber, 1964) and the isotopic composition of metasomatizing fluids (δ¹⁸O_{SMOW}=9‰ and δ¹³C_{PDB}=-8‰) are also shown for an open and closed system. The open and closed systems are marked with solid and dashed curves, respectively.

In Figure 11 the isothermal curves of water-rock exchange (within the temperature range of 150-200 °C) are shown for different water/rock ratios as a function of $X_{\text{H}_2\text{CO}_3}$. The values between 0.3 and 0.5 indicate an increase in H_2CO_3 of the hydrothermal fluid at the time of replacement of carbonates by iron ores. These curves show that by increasing the exchange rate, the lighter carbon and oxygen isotopes will prevail. The curves drawn for open system also indicate isotopic exchange between host carbonates and hydrothermal fluids. It is assumed that the CO_2 ($\approx\text{H}_2\text{CO}_3$) content of the hydrothermal fluids was low during the replacement of carbonates. While H_2CO_3 was the dominant carbon species in the fluids, and its value gradually increased from 0.3 to 0.5 mole during alteration of the wall rocks, a mole fraction of <0.5 ($X_{\text{H}_2\text{CO}_3}=0.3-0.5$) could be assumed for H_2CO_3 during the fluid/rock interaction processes. There is a negative correlation between carbon and oxygen isotopes in calcite at Gharkohneh that could be owing to progressive temperature decrease during slow and gradual egression of CO_2 and conversion of H_2CO_3 to HCO_3^- during the deposition of calcite at temperatures around 150 °C (Zheng, 1990).

Mode of formation mechanism for the Gharkohneh iron deposit

The Gharkohneh iron deposit is stratabound and carbonate-hosted. Mineralization is mainly of vein/veinlet-type and structurally controlled by fault and fractured zones. The mode of mineralization is almost similar to those of the Pivehzhah in Iran (Najafzadeh Tehrani et al., 2018a), SieraMenera and Marquesado in Spain (Fernández-Nieto et al., 2003; Torres, 2006). These deposits are widely distributed in carbonates and some in metamorphic rocks.

Some of the important characteristics of the fluid inclusions entrapped at low depths (<1 km) and brittle epithermal environments are their small sizes, low to moderate TH values (from <100 °C up to 300 °C), abundance of 2-phase (L+V) inclusions, and the lack of daughter solid phases (Wilkinson, 2001). These characteristics are in agreement with the petrography and the microthermometric data of the fluid inclusions.

Structural, textural, and mineralogical data along with field relations provided sufficient evidence for the Gharkohneh iron ores to be categorized as an epigenetic deposit, which was developed during two distinct hypogene and supergene stages within the metamorphosed and folded sedimentary rocks.

The mineralization occurred mainly at the margin of the fault zone (Figure 3), which may indicate that the brecciated zone provided a permeable conduit for the ascending Fe-rich hydrothermal fluids. One of the reasonable sources for iron might be the igneous intrusive

body existing at depth, a small apophysis of which is also exposed at the surface within the Silurian sandstone in a distance about 700 m west of the study area. It contains ferromagnesian minerals and suffered chloritization. Nonetheless, determination of the precise source of iron requires even more detailed studies.

It is likely that the hydrothermal solutions were enriched in iron by leaching it from magmatic rocks, and precipitated the iron minerals (primary oxides and sulfides) upon ascending through the permeable fault zone within the reactive carbonate rocks (Hemley and Hunt, 1992).

Upon ascending and interaction with reactive carbonate rocks along the passage ways furnished by fault breccia zones (Figure 3b), such Fe-rich hypogene hydrothermal fluids precipitated iron oxides and sulfides as both replacement (Figure 5c) and open-space filling in the fault breccia zones (Figure 3b). The presence of replacement texture in the carbonate rocks shows that the reaction of the ore-forming fluids with the host carbonates and hence, the increase in pH has resulted in the instability of metallic complexes and ultimately, the deposition of the iron ores (Barnes, 1997). However, the sulfide and magnetite content of the surface outcrops are very low due to the severe weathering processes.

Fluid inclusion and isotopic (C and O) data demonstrated that the late hypogene mineral phases (pyrite veins and calcite) were formed by moderate-temperature, and low to moderate-salinity hydrothermal fluids. According to the theoretical models of water/rock interactions, the late hydrothermal minerals might have formed mainly within the temperature range of 150- 200 °C (Figure 11) and at W/R ratios between 1 and 5. These conditions are consistent with the principal microthermometric results of fluid inclusions and strongly suggest moderate temperatures and slow velocities for fluid circulation through open fractures. These characteristics probably explain the similarity of isotopic values in the host carbonates and the hydrothermal calcites. The relatively low W/R ratios caused that the carbon and oxygen isotopic composition of the host rocks preponderate over those of the fluids.

The supergene stage commenced once the hypogene sulfides were exposed to the vadose zone and oxidized by the reaction with oxygenated waters of meteoric origin (Bigham and Nordstrom, 2000). The extensive hematite and goethite mineralization with dominant skeletal, pseudomorph, relict replacement, and marginal replacement textures indicates that goethite was the first supergene mineral phase formed through the oxidation of ferrous iron by the supergene solutions (Najafzadeh Tehrani et al., 2018b). The presence of hematite and goethite in the karstic parts at Gharkohneh also show considerable similarity with the oxidized section of the

Sierra Menera deposit and the gossans capping deposits in the Iberian Pyrite Belt (Fernández-Nieto et al., 2003; Velasco et al., 2013).

CONCLUSION

The Gharkohneh iron deposit was developed within the Devonian carbonate host rocks by two processes, (1) the hypogene and (2) the supergene. The principal iron minerals of the hypogene zone are pyrite and magnetite, while the supergene zone is characterized by the dominance of hematite and goethite. The late ore-forming hydrothermal fluids had low to moderate temperature and salinity during precipitation of hypogene minerals, which occurred at low water/rock ratios (1-5). The similarity of $\delta^{18}\text{O}_{\text{SMOW}}$ and $\delta^{13}\text{C}_{\text{PDB}}$ values of the hydrothermal calcite with those of the host carbonates suggests that H_2CO_3 in the ore-forming fluids was derived from the surrounding carbonate rocks. The $\delta^{18}\text{O}$ and $\delta^{13}\text{C}$ values of the host carbonates are slightly lower than those of the marine sediments, which may be due to the hydrothermal alteration or metasomatic processes. Based upon carbon and oxygen isotopic data, petrographic examinations and geochemical investigations, this deposit is classified as a hydrothermal iron deposit. The presence of boxwork, replacement, skeletal, colloform and botryoidal textures indicate the extensive replacement of sulfides by iron-oxides and hydroxides in the supergene oxidized zone. Geochemical data revealed that the ores contain major oxides of Fe, S and Mn accompanied by minor amounts of Pb, Zn, Cu, Co, Ni and V.

ACKNOWLEDGEMENTS

Authors would like to express their thanks for financial and experimental supports provided by the Research Deputy Bureau of the University of Tabriz (Iran), University of Basque Country (Spain), and Iranian Mineral Processing Research Center (Karaj). Also, authors would like to state their appreciation to Prof. I. Yusta (Faculty of Sciences and Technology, University of Basque Country) for letting us perform XRF analyses and to Dr. F. Tornos (Spanish National Research Council, Madrid) for facilitating the oxygen and carbon stable isotopic analyses. Our gratitude is further extended to the anonymous reviewers, who have reviewed the manuscript and made critical comments and fruitful suggestions.

REFERENCES

- Aghanabati A., 2004. Geology of Iran. Geological Survey of Iran, Tehran, Iran, (Persian), 538 pp.
- Ahmad S., and Rose A., 1980. Fluid inclusions in porphyry and skarn ore at Santa Rita, New Mexico. *Economic Geology* 75, 229-250.
- Alavi M., 1991. Sedimentary and structural characteristics of the Paleo-Tethys remnants in northeastern Iran. *Geology Society America Bulletin* 103, 983-992.
- Alavi M., 1992. Thrust tectonics of the Binalood region, NE Iran. *Tectonics* 11, 360-70.
- Barnes H.L., 1997 (Eds.). *Geochemistry of hydrothermal ore deposit*, 2nd edition. John Wiley and Sons Inc, New York, 972 pp.
- Bigham J.M. and Nordstrom D.K., 2000. Iron and aluminium hydroxy sulfates from acid sulfate waters. In: Alpers C.N., Jambor J.L., Nordstrom D.K. (Eds.), *Sulfate Minerals-Crystallography, Geochemistry and Environmental Significance*, Review. *Mineralogy and Geochemistry* 40, Mineral Society, American Washington, DC, 351-403.
- Bodnar R.J., Reynolds T.J., Kuehn C.A., 1985. Fluid inclusion systematics in epithermal systems. In: Berger B.R., Bethke P.M. (Eds.) *Geology and Geochemistry of Epithermal Systems*, *Reviews in Economic Geology* 2, 73-97.
- Bonyadi Z., Davidson G.J., Mehrabi B., Meffre S., Ghazban F., 2011. Significance of apatite REE depletion and monazite inclusions in the brecciated Se-Chahun iron oxide-apatite deposit, Bafq district, Iran, insights from paragenesis and geochemistry. *Chemical Geology* 281, 253-269.
- Boomeri M., Ishiyama D., Mizuta T., Matsubaya O., Lentz D.R., 2010. Carbon and oxygen isotopic systematics in calcite and dolomite from the Sangan Iron Skarn Deposit, Northeastern Iran. *Journal of Science, Islamic Republic of Iran* 21, 213-224.
- Bottinga Y., 1969. Calculated fractionation factors for carbon and hydrogen isotope exchange in the system calcite-carbon dioxide-graphite-methane-hydrogen-water vapor. *Geochemica Cosmochimica et Acta* 33, 49-64.
- Craig H., 1957. Isotopic standards and isotopic correction factors for mass spectrometric analysis of carbon dioxide. *Geochimica et Cosmochimica Acta* 12, 133-149.
- Davoudzadeh M., Aghanabati M., Shahrabi M., 1975. An organic phase of mid-Jurassic age in northeast Iran Binalood Mountain range. *Neues Jahrb. Mineral. Geology Palaeontol. Beil* 162, 137-163.
- Fernández-Nieto C., Torres-Ruiz J., Pérez I.S., González I.F., López J.G., 2003. Genesis of Mg-Fe carbonates from the Sierra Menera magnesite-siderite deposits, Northeast Spain. Evidence from fluid inclusions, trace elements, rare earth elements, and stable isotope data. *Economic Geology* 98, 1413-1426.
- Forster H. and Jafarzadeh A., 1994. The Bafq mining district in central Iran; a highly mineralized Infracambrian volcanic field. *Economic Geology* 89, 1697-1721.
- Folk Robert L., 1962. Petrography and origin of the Silurian Rochester and McKenzie Shales, Morgan County, West Virginia. *Journal of Sedimentary Research* 32, 3.
- Ghorbani M., 2013. *The economic geology of Iran: mineral deposits and natural resources*. New York, Springer Dordrecht Heidelberg, 581 pp.
- Hall D.L., Sterner S.M., Bondar R.J., 1988. Freezing point

- depression of NaCl-KCl-H₂O solutions. *Economic Geology* 93, 197-202.
- Heidarian H., Alirezaei S., Lentz D.R., 2017. Chadormalu Kiruna-type magnetite-apatite deposit, Bafq district, Iran. Insights into hydrothermal alteration and petrogenesis from geochemical, fluid inclusion, and sulfur isotope data. *Ore Geology Review* 83, 43-62.
- Hemley J. and Hunt J., 1992. Hydrothermal ore-forming processes in the light of studies in rock-buffered systems II, Some general geologic applications. *Economic Geology* 87, 23-43.
- Holzer H.F. and Moemen Zadeh H., 1969. Report on reconnaissance of granite margins in the Mashhad area, Khorasan province, northeastern Iran. Tehran, Geological survey of Iran, 41 pp. (Internal Report).
- Jami M., Dunlop A.C., Cohen D.R., 2007. Fluid inclusion and stable isotope study of the Esfordi apatite-magnetite deposit, Central Iran. *Economic Geology* 102, 1111-1128.
- Keith M. and Weber J.N., 1964. Carbon and oxygen isotopic composition of selected limestones and fossils. *Geochemical et Cosmochimica Acta* 28, 1787-1816.
- Lammerer B., Langheinrich G., Manutchehr Danai M., 1983. The tectonic evolution of the Binaloud NE-Iran, Geodynamic project Geotraverse in Iran, in geodynamic project in Iran, Geological Survey of Iran, Tehran, 51, 91-102 (Final report).
- Mohseni S. and Aftabi A., 2015. Structural, textural, geochemical and isotopic signatures of synglaciogenic Neoproterozoic banded iron form at iron BIFs at Bafq mining district BMD, Central Iran. The possible Ediacaran missing link of BIFs in Tethyan metallogeny. *Ore Geology Review* 71, 215-236.
- Nabatian G., Ghaderi M., Corfu F., Neubauer F., Bernroider M., Prokofiev V., Honarmand M., 2014. Geology, alteration, age, and origin of iron oxide-apatite deposits in Upper Eocene quartz monzonite, Zanjan district, NW Iran. *Mineralium Deposita* 49, 217-234.
- Nabavi M., 1976. An introduction to the geology of Iran. Tehran, Geological survey of Iran, Tehran, (Persian), 109 pp.
- Najafzadeh Tehrani P., Calagari A.A., Abedini A., Mazlumi A., 2013. Geological, mineralogical, alteration features, rare earth elements (REEs) geochemistry of Neyzar Iron deposit, Southwest of Mashhad, Northeast Iran. *Iranian Society of Crystallography and Mineralogy*, (Persian with English abstract) 21, 229-242.
- Najafzadeh Tehrani P., Calagari A.A., Velasco Roldan F., Simmonds V., Siahcheshm K., 2018a. C and O stable isotopes and rare earth elements in the Devonian carbonate host rock of the Pivehzhah iron deposit, NE Iran. *Geologica Acta* 16, 125-148.
- Najafzadeh Tehrani P., Calagari A.A., Velasco Roldan F., Yusta I., 2018b. Geochemistry, texture, and mineralogy of supergene zones of iron deposits from the Binaloud zone, NE Iran, *Neues Jahrbuch für Mineralogie Abhandlungen* 195, 211-225.
- Ohmoto H., 1986. Stable isotope geochemistry of ore deposits. In: Walley J.W., Taylor H.P., O'Neil J.R. (Eds.). *Stable Isotopes in High Temperature Geological Processes*. Mineral Society America 16, 491-570.
- Ohmoto H., 1972. Systematics of Sulfur and carbon isotopes in hydrothermal ore deposits. *Economic Geology* 67, 551-579.
- Ohmoto H. and Rye R.O., 1979. Isotopes of sulfur and carbon. In: Barnes, H.L. (Ed.). *Geochemistry of Hydrothermal Ore Deposits*, New York, Wiley, 509-567.
- O'Neil J. R., Clayton R.N., Mayeda T.K., 1969. Oxygen isotope fractionation in divalent metal carbonates. *The Journal of Chemical Physics* 51, 5547- 5558.
- Pourlatifi A., AlaviNaieni M., Shojae N., 2001. Geological map of Torghabeh, Geological survey of Iran, Geological map of Iran 1:100,000, series sheet no 7852.
- Rye R.H. and Ohmoto H., 1974. Sulfur and carbon isotopes and ore genesis. A review. *Economic Geology* 69, 826-842.
- Spies O., Lensch G., Mihem A., 1983. Chemistry of post-ophiolitic tertiary volcanic between Sabzevar and Quchan, NE Iran, In Almassi. A. ed., *Geodynamic project geotravers in Iran*, Geological survey of Iran, Tehran 51, 247-266.
- Steele-MacInnis M., Bodnar R.J., Naden J., 2011. Numerical model to determine the composition of H₂O-NaCl-CaCl₂ fluid inclusions based on microthermometric and microanalytical data. *Geochimica et Cosmochimica Acta* 75, 21-40.
- Taofa Z., Mingan W., Yu F., Chao D., Feng Y., Lejun Z., Jun L., Bing Q., Pirajno F., Cooke D.R., 2011. Geological, geochemical characteristics and isotope systematics of the Longqiao iron deposit in the Lu-Zong volcano-sedimentary basin, Middle-Lower Yangtze Changjiang River Valley, Eastern China. *Ore Geology Review* 43, 154-169.
- Taylor H.P., Frechen J., Degens E.T., 1967. Oxygen and carbon isotope studies of carbonatites from the Laacher See District, West Germany and the Alnö District, Sweden. *Geochimica et Cosmochimica Acta* 31, 407-3.
- Torab F. M., 2008. Geochemistry and metallogeny of magnetite apatite deposits of the Bafq Mining District, Doctoral thesis, Faculty of Energy and Economic Sciences, Clausthal University of Technology, Germany, 144 pp.
- Torres-Ruiz J., 2006. Geochemical constraints on the genesis of the Marquesado iron ore deposits, Betic Cordillera, Spain. REE, C, O, and Sr isotope data. *Economic Geology* 101, 667-677.
- Velasco F., Herrero J.M., Suárez S., Yusta I., Alvaro A., Tornos F., 2013. Supergene features and evolution of gossans capping massive sulphide deposits in the Iberian Pyrite Belt. *Ore Geology Review* 53, 181-203.
- Wauschkuhn A., Ohnsmann M., Momenzadeh M., 1984. The Paleozoic rocks of the South Binalud Mountains, NE Iran, an exploration target for Fe, Pb, Zn and Ba. *Neues Jahrbuch für Mineralogie Abhandlungen* 168, 479-489.
- Wendt J., Kaufmann B., Belka Z., Farsan N., Karimi Bavandpur A., 2005. Devonian/Lower Carboniferous stratigraphy, facies patterns and palaeogeography of Iran. Part II. Northern and

- central Iran. *Acta Geology Polonica* 55, 31-97.
- Wilkinson J., 2001. Fluid inclusions in hydrothermal ore deposits. *Lithos* 55, 229-272.
- Zhang Y.G. and Frantz J.D., 1987. Determination of the homogenization temperatures and densities of supercritical fluids in the system NaCl-KCl-CaCl₂-H₂O using synthetic fluid inclusions. *Chemical Geology* 64, 335-350.
- Zheng Y-F., 1990. Carbon-oxygen isotopic covariation in hydrothermal calcite during degassing of CO₂. *Mineralium Deposita* 25, 246-50.
- Zheng Y-F. and Hoefs J., 1993. Carbon and oxygen isotopic conversations in hydrothermal calcites. *Mineralium Deposita* 28, 79-89.
- Zhou J.-X., Huang Z.-L., Lv Z.-C., Zhu X.-K., Gao J.-G., Mirnejad H., 2014. Geology, isotope geochemistry and ore genesis of the Shanshulin carbonate-hosted Pb-Zn deposit, southwest China. *Ore Geology Review* 63, 209-225.



This work is licensed under a Creative Commons Attribution 4.0 International License CC BY. To view a copy of this license, visit <http://creativecommons.org/licenses/by/4.0/>

